



SUPA, School of Physics and Astronomy  
Experimental Particle Physics Group  
Kelvin Building, University of Glasgow,  
Glasgow, G12 8QQ, Scotland  
Telephone: +44 (0)141 330 2000 Fax: +44 (0)141 330 5881

## A Neutrino Factory Toroidal MIND at Large $\theta_{13}$

R. Bayes<sup>1</sup>, A. Bross<sup>2</sup>, A. Cervera-Villanueva<sup>3</sup>, M. Ellis<sup>4</sup>, T. Ghosh<sup>3</sup>, A. Laing<sup>1</sup>, F.J.P. Soler<sup>1</sup>, R. Wands<sup>2</sup>

<sup>1</sup> School of Physics and Astronomy, University of Glasgow, Glasgow, G12 8QQ, UK

<sup>2</sup> Fermilab, P.O. Box 500, Batavia, IL 60510-5011, USA

<sup>3</sup> IFIC and Universidad de Valencia, Valencia, Spain

<sup>4</sup> Westpac Institutional Bank, NSW, Australia

### Abstract

A neutrino factory has unparalleled physics reach for the discovery and measurement of CP violation in the neutrino sector. A far detector for a neutrino factory must have good charge identification with excellent background rejection and a large mass. An elegant solution is to construct a magnetized iron neutrino detector along the lines of MINOS, where iron plates provide a magnetic field and scintillator planes provide 3D space points. In this presentation, the current status of a simulation of MIND for a neutrino factory will be discussed, focussing on the ramifications of the recent measurement of large  $\theta_{13}$ . Particular detail will be applied to results using the new baseline 10 GeV neutrino factory configuration. A summary of the expected detector performance from the current reconstruction will be given with the resulting sensitivities.

*NuFACT 2012, International Conference on Neutrino Factories, Super Beams, and Beta Beams  
Williamsburg, VA, USA*

	Store $\mu^+$	Store $\mu^-$
Golden Channel	$\nu_e \rightarrow \nu_\mu$	$\bar{\nu}_e \rightarrow \bar{\nu}_\mu$
$\nu_e$ Disappearance Channel	$\nu_e \rightarrow \nu_e$	$\bar{\nu}_e \rightarrow \bar{\nu}_e$
Silver Channel	$\nu_e \rightarrow \nu_\tau$	$\bar{\nu}_e \rightarrow \bar{\nu}_\tau$
Platinum Channel	$\bar{\nu}_\mu \rightarrow \bar{\nu}_e$	$\nu_\mu \rightarrow \nu_e$
$\nu_\mu$ Disappearance Channel	$\bar{\nu}_\mu \rightarrow \bar{\nu}_\mu$	$\nu_\mu \rightarrow \nu_\mu$
Dominant Oscillation	$\bar{\nu}_\mu \rightarrow \bar{\nu}_\tau$	$\nu_\mu \rightarrow \nu_\tau$

Table 1: Oscillation channels observable at a neutrino factory.

## 1 Introduction

The discovery of large  $\theta_{13}$  by Daya Bay [An et al.(2012)] and others [Ahn et al.(2012), Okumura(2012), Yang(2011)] requires a shift in the priorities of the planning for the next generation neutrino experiments, including neutrino factory [Choubey et al.(2011)]. This discovery focusses the neutrino factory long baseline physics program on the optimized measurement of CP violation. The optimal experimental design consists of a single detector at a baseline of 2000 km with a stored muon energy of 10 GeV. This supersedes a two detector configuration with baselines of 4000 and 7500 km and a stored muon energy of 25 GeV which was required to resolve  $\delta_{CP}$  degeneracies in the case of small  $\theta_{13}$ .

A neutrino factory offers unique physics opportunities because of the clean neutrino beam generated by muon decays at an extremely high rate. The content of the beam is precisely known as 50%  $\nu_e(\bar{\nu}_\mu)$  and 50%  $\bar{\nu}_\mu(\nu_\mu)$ , presenting six different channels for long baseline oscillations (see Table 1). The most easily detected channels are those where there is a  $\mu^\pm$  in the final state of a neutrino charge current (CC) interaction. The significance of a measurement is limited by the ability to remove neutral current (NC) interactions and resolve the signal muon charge as a primary source of background with the opposite charge to the signal. For a neutrino factory, a magnetized iron neutrino detector (MIND) is the favoured far detector [Cervera et al.(2010), Bayes et al.(2012)] because it has excellent charge identification capabilities coupled with an easily scalable fiducial mass. These proceedings describe an optimization of the NF golden channel oscillation analysis,  $\nu_e(\bar{\nu}_e) \rightarrow \nu_\mu(\bar{\nu}_\mu)$ , in a realistic MIND.

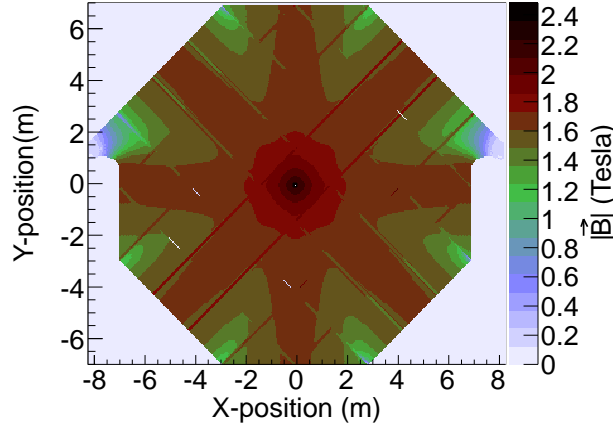


Figure 1: Magnetic field map of detector.

## 2 Simulation Overview

The neutrino factory MIND is an iron-scintillator calorimeter, analogous to MINOS[Michael et al.(2008)], consisting of alternating steel and scintillator planes. The detector has an octagonal cross-section 14 m $\times$ 14 m with triangular support structures on either side of the steel plates. To produce the planned 100 kTon fiducial mass, this detector needs to be 140 m in length. The magnetic field is induced in the 3 cm thick steel planes using 120 kA of current to be carried by one or more turns of a 7 cm diameter super conducting transmission line (STL)[Ambrosio et al.(2001)]. The magnetic field magnitude from a simulated detector plate is shown in Fig. 1. The majority of magnetic field lines point in the azimuthal direction, which focus positive charges toward the

Event Cut	Description	Signal Eff		Background ( $\times 10^3$ )	
		$\bar{\nu}_\mu$	$\nu_\mu$	$\bar{\nu}_\mu$	$\nu_\mu$
Successful Track Fit	Failed Kalman reconstruction of event removed	85.3%	71.2%	291( $\bar{\nu}_e$ )	301( $\nu_e$ )
Fiducial	Event vertex more than 1.5 m from end of detector	84.9%	70.8%	288( $\bar{\nu}_e$ )	298( $\nu_e$ )
Maximum Momentum	Muon momentum less than $1.6 \times E_\mu^{stored}$	84.0%	69.4%	253( $\bar{\nu}_e$ )	266( $\nu_e$ )
Fitted Proportion	60% of track nodes used in final fit.	83.8%	68.7%	238( $\bar{\nu}_e$ )	249( $\nu_e$ )
Track Quality	$\log(P(\sigma_{q/p}/(q/p) CC)/P(\sigma_{q/p}/(q/p) NC)) > -0.5$	80.7%	64.0%	66( $\nu_\tau$ )	76( $\nu_e$ )
CC Selection	$\log(P(N_{hit} CC)/P(N_{hit} NC)) > 1.0$	79.4%	57.5%	3.4( $\nu_\tau$ )	3.7( $\nu_e$ )
Kinematic	$Q_t > 0.15 GeV$	74.1%	54.7%	2.4( $\nu_\tau$ )	0.9( $\bar{\nu}_\tau$ )

Table 2: Cuts used in the selection of good events from the simulation with the integrated signal efficiencies and leading backgrounds after each cut.

centre of the detector by default. The scintillator planes are a 2 cm thick lattice of 1 cm $\times$ 3.5 cm scintillator bars in the  $x$  and  $y$  direction to measure a 3D space point between each steel plane with a 1 cm position resolution.

This geometry was simulated in GEANT4[Allison et al.(2006)] using the QGSP\_BERT physics list for hadron interactions. The specifications of the detector geometry was set up so that it is easily altered for optimization studies and to test detector variations. Neutrino events were simulated using the GENIE event generator[Andreopoulos et al.(2010)]. Each of the simulated events was subject to a simple digitization wherein the positions of the hits were smeared, the energy deposition of each hit was attenuated, assuming a 5 m attenuation length, and the hits were clustered into 3.5 cm $\times$ 3.5 cm units corresponding to the transverse width of the scintillator bars.

Tracks were identified using a Kalman filtering algorithm, or, if the longest set of single occupancy planes is less than 5 planes long, a Cellular Automaton method[Cervera et al.(2010)]. The identified tracks were subjected to a Kalman fitting algorithm to determine the momentum and the charge of the track based on its curvature. The algorithms used for this reconstruction are contained in the RecPack software package[Cervera-Villanueva et al.(2004)].

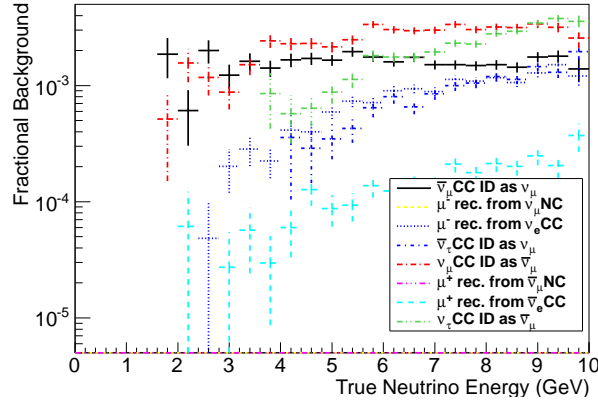


Figure 2:  $\mu^+$  focussed background.

### 3 Analysis

Subsequent analysis was done to separate the  $\nu_\mu(\bar{\nu}_\mu)$ CC signal events from the backgrounds. This was done through the successive application of a set of seven cuts; four cuts to remove poorly reconstructed events and three to explicitly differentiate CC signal events from background. These cuts and their impact on the signal and background are summarized in Table 2.

The most effective cuts were on the Track Quality and the CC selection. Both used a similar formalism to identify muons and reject backgrounds using the logarithm of the ratio of the probability that the given event was a charge current or neutral current event. For the track quality cut the probability was defined using the distribution of the scaled error in the measurement of the charge divided by the momentum,  $\sigma_{q/p}/(q/p)$ . The probability used for the CC selection cut is based on the distribution of the number of hits in a sample of CC trajectories and NC trajectories. The combination of these cuts suppressed the NC backgrounds to below the level of the statistics (parts in  $10^{-6}$ ) while all remaining backgrounds were suppressed by parts in  $10^{-3}$ , as shown in Fig 2 for a positive focussing field and Fig. 3 for a negative focussing field. The reconstruction

efficiencies were at or above 50% after these cuts were applied. The detector performance depended on whether the detector field focused positive or negative charges as shown in Fig. 4 and Fig. 5, as a result of reconstructing different inelasticity distributions in  $\nu_\mu$  and  $\bar{\nu}_\mu$  CC samples.

A multivariate analysis is under development for the MIND analysis. This analysis uses a larger subset of variables than those described above to identify and remove neutral current events, including the mean and variation of energy deposition along reconstructed tracks. Such a method should be able to select muons with a lower energy threshold than the existing cuts.

## 4 Sensitivity to $\delta_{CP}$

The detector response was used to determine the sensitivity of a neutrino factory to CP violation in muon neutrino appearance channel. A set of migration matrices, one for the NC background and one for each of the oscillation channels, were defined using the flux normalized response as a function of the true neutrino energy versus the reconstructed neutrino energy. The fluxes and oscillation probabilities were calculated using the Neutrino Tool Suite (NuTS)[Burguet-Castell et al.(2001)]. Both  $\theta_{13}$  and  $\delta_{CP}$  were fit simultaneously by minimizing

$$\begin{aligned} \chi^2 = 2 \times \sum_e^{E_\mu} & \left\{ AxN_+^e(\theta_{13}, \delta_{CP}) - n_+^e \right. \\ & + n_+^e \log \left( \frac{n_+^e}{AxN_+^e(\theta_{13}, \delta_{CP})} \right) \\ & \left. + AN_-^e(\theta_{13}, \delta_{CP}) - n_-^e \right\} \end{aligned}$$

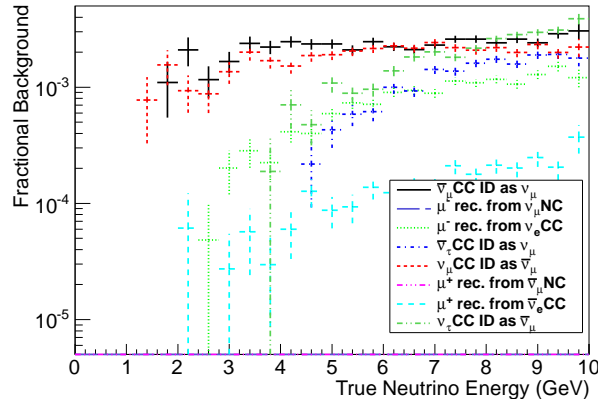


Figure 3:  $\mu^-$  focussed background.

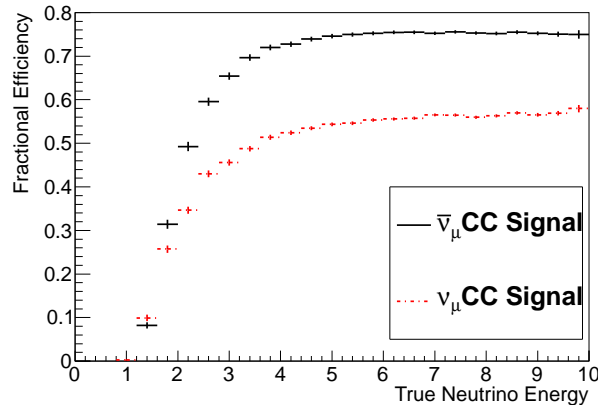


Figure 4:  $\mu^+$  focussing detector efficiency.

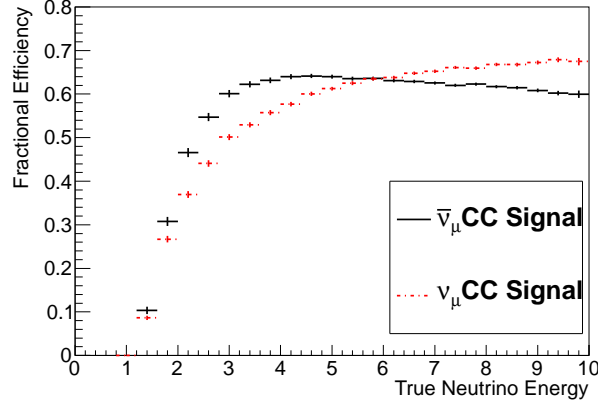


Figure 5:  $\mu^-$  focussing detector efficiency.

$$\begin{aligned}
 & + n_-^e \log \left( \frac{n_-^e}{A_j N_-^e(\theta_{13}, \delta_{CP})} \right) \\
 & + \frac{(A-1)^2}{\sigma_A^2} + \frac{(x-1)^2}{\sigma_x^2} \Big\} \quad (1)
 \end{aligned}$$

where  $n_i^e$  is the "data" for an energy bin  $e$ , assuming a detector baseline of 2000 km from stored muons with charge  $i$ , and  $N_i^e$  is the prediction for the same bin. Two systematic uncertainties were assumed to dominate and appear explicitly in this  $\chi^2$  formulation; an uncertainty in the total number of interactions in the detector ( $\sigma_A$ ), believed to be 1%, and the uncertainty in the ratio between  $\nu_\mu$  and  $\bar{\nu}_\mu$  cross-sections ( $\sigma_x$ ), also assessed as 1%. As the ratio of stored muon charges is not known for the apparatus and the ratio does not affect the final physics results, it is assumed that  $5 \times 10^{20}$  muons of both charges will decay in the storage ring per year.

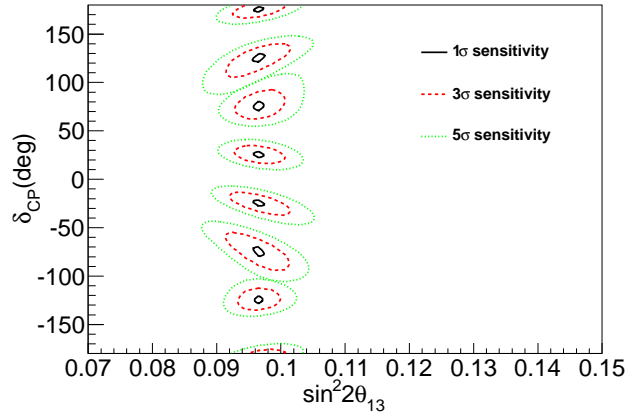


Figure 6: Fits to "data" assuming arbitrary  $\delta_{CP}$  at  $\theta_{13} = 9^\circ$ .

$\chi^2$  contours derived from the Eq. 1 as functions of  $\sin^2 2\theta_{13}$  and  $\delta_{CP}$  for 10 years of running are shown in Fig. 6 assuming various true values for  $\delta_{CP}$  and that the  $\theta_{13} = 9^\circ$ . With the measurement of  $\theta_{13}$  the precision of the experiment to  $\delta_{CP}$  has become the primary figure of merit for the performance of the experiment. The one standard deviation error contour as a function of  $\delta_{CP}$  is shown in Fig. 7 assuming the systematic uncertainties to be 1% and assuming  $\sigma_x = 3\%$  and  $\sigma_A = 2.5\%$ , illustrating the sensitivity of the neutrino factory to variation in the systematics. The experiment is not sensitive to reversing the detector field polarity as the sensitivity contours are identical for positive and negative charge focussing magnetic fields.

The results using a toroidal magnetic field have backgrounds that are an order of magnitude larger than those achieved for interim analyses with a dipole field[Bayes et al.(2012)]. The reduction in background does not affect the experimental sensitivity, however. Gains in the experimental sensitivity will likely not be made by reducing background or improving efficiency without increased knowledge of the energy threshold of the experiment.

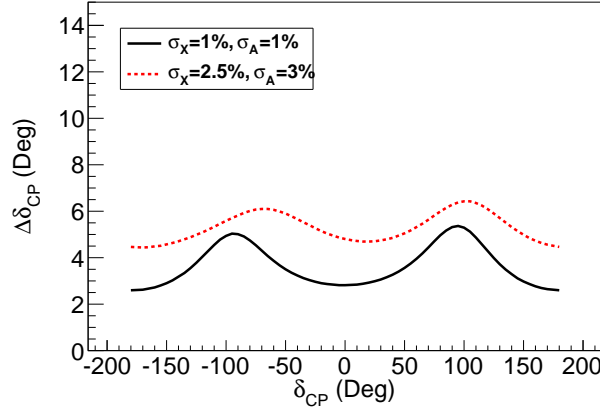


Figure 7: Precision in  $\delta_{CP}$  as a function of  $\delta_{CP}$ .

## 5 Conclusions

The simulation of the neutrino factory MIND has made a great deal of progress in the last year. The simulation has made a complete change to the GENIE event generator following the example of MINOS and others. A realistic octagonal geometry has been introduced with a corresponding magnetic field simulation. These modifications were accompanied by improvements in the track reconstruction to accommodate the new magnetic field map. However there is still work in progress. The reconstruction must be made to reconstruct hadronization and the analysis is being updated to use a multi-variate method for the rejection of neutral current events. Preliminary analyses show that a neutrino factory with a MIND can achieve a precision in  $\delta_{CP}$  between  $2.5^\circ$  and  $4.5^\circ$ .

## 6 Acknowledgements

This work was completed with the support of the European Commission Framework Program 7 Design Study: EUROnu, Project Number 212372, the Science and Technology Facilities Council (UK), the Spanish Ministry of Education and Sciences, and the Department of Energy (USA).

## References

- [An et al.(2012)] F. An, et al., *Phys.Rev.Lett.* **108**, 171803 (2012), 1203.1669.
- [Ahn et al.(2012)] J. Ahn, et al., *Phys.Rev.Lett.* **108**, 191802 (2012), 1204.0626.
- [Okumura(2012)] K. Okumura, *AIP Conf.Proc.* **1441**, 451–453 (2012).
- [Yang(2011)] T.-J. Yang, *Int.J.Mod.Phys.* **A26**, 179–189 (2011).
- [Choubey et al.(2011)] S. Choubey, et al., Interim Design Report, Tech. Rep. IDS-NF-020, IDS-NF (2011).
- [Cervera et al.(2010)] A. Cervera, et al., *Nucl. Instrum. Meth. A* **624**, 601–614 (2010), [arXiv:1004.0358\[hep-ex\]](#).
- [Bayes et al.(2012)] R. Bayes, A. Laing, F. Soler, A. C. Villanueva, J. G. Cadenas, et al., *Phys. Rev. D* **86**, 093015 (2012), URL <http://link.aps.org/doi/10.1103/PhysRevD.86.093015>, 1208.2735.
- [Michael et al.(2008)] D. Michael, et al., *Nucl.Instrum.Meth.* **A596**, 190–228 (2008), 0805.3170.
- [Ambrosio et al.(2001)] G. Ambrosio, et al., Design study for a staged very large hadron collider, Tech. rep. (2001).
- [Allison et al.(2006)] J. Allison, et al., *Nuclear Science, IEEE Transactions on* **53**, 270 –278 (2006), ISSN 0018-9499.
- [Andreopoulos et al.(2010)] C. Andreopoulos, et al., *Nucl. Instrum. Meth. A* **614**, 87–104 (2010), [arXiv:0905.2517\[hep-ph\]](#).

[Cervera-Villanueva et al.(2004)] A. Cervera-Villanueva, et al., *Nucl. Instrum. Meth. A* **534**, 180–183 (2004).

[Burguet-Castell et al.(2001)] J. Burguet-Castell, et al., *Nucl. Phys. B* **608**, 301–318 (2001), [hep-ph/0103258](#).